International Journal of Biochemistry, Bioinformatics and Biotechnology Studies
Vol.7, No.2, pp.21-30, 2022
Print ISSN: 2397-7728(Print)
Online ISSN: 2397-7736(Online)

Antimicrobial application of Silver Nanoparticles Supported on $Ti_{1-x}Ce_xO_2$: Synthesis and Morphological Characterization

América A. Mondragón H.[1], Roberto Guerra G.[1], Ramiro Escudero G.[2] *, José Luis Rivera[1]

Universidad Michoacana de San Nicolás de Hidalgo. Santiago Tapia 403. C.P.58000. Morelia, Michoacán, México. [1] Basic Sciences and Engineering. [2] Institute of Research in Metallurgy and Materials.

*Author to whom correspondence should be addressed

Citation: América A. M. H., Roberto G. G., Ramiro E. G., José LR. (2022) Antimicrobial application of Silver Nanoparticles Supported on Ti1-xCexO2: Synthesis and Morphological Characterization, International Journal of Biochemistry, Bioinformatics and Biotechnology Studies, Vol.7, No.2, pp.21-30

ABSTRACT: *Water pollution affects ecosystems including humans, water reserves for human consumption are increasingly scarce and disinfection methods are expensive and ineffective. In this work, a material based on TiO_2 was synthesized using the sol-gel method, and then doped with CeO_2; Silver was added to the synthesized material by the incipient moisture method, to provide the bactericidal effect against Salmonella Typhimurium strains. The experimental results show the presence of crystalline phases of TiO_2-Ce and deposits of Ag. The combination of Ti, Ce, and Ag in the $Ag/Ti_{0.96}Ce_{0.04}O_2$, worked as a bactericidal material for Salmonella Typhimurium; the silver content of 4% (w/w) was sufficient to inhibit bacteria. This could be because cerium and titanium break down the cell membrane, which makes silver easily interact with the nucleus of bacteria.The textural results show the diameter of the pores in all samples ranges from 2 to 50 nm (mesoporous solid). On the other hand, the rough morphology of the nanoparticles could enhance the antibacterial efficacy because it contributes to the rupture of the membranes of the aforementioned bacteria.*

KEYWORDS: Silver nanoparticles, Salmonella Typhimurium, Synthesis, Water pollution, Sol-gel method, Photoactivity, Photocatalysis, Anatase.

INTRODUCTION

Water is essential for life, a good supply guarantees great health benefits. According to the World Health Organization (WHO), around 5 million people die each year from conditions derived from water contamination, 50% of these deaths are associated with gastrointestinal infections. The greatest bacterial risks are due to the ingestion of water contaminated with human and animal feces (Grabow, W.O.K., 1996; George et al., 2001; Fenwick, A., 2006; WHO, 2008). The use of disinfectants is crucial to reduce pathogens in personal hygiene, in wastewater treatment, and during urban use in general (McDonnell, G., and Russell, A.D., 1999). In recent years, semiconductor photocatalysis has been studied for pollutant removal treatments in water and air (Pant et al., 2016; Opoku et al., 2017). Titanium dioxide (TiO_2) has been used as a photocatalyst for antimicrobial purposes (Liou, J.W., and Chang, H.H., 2012), due to its high photoactivity, good chemical stability, low cost, and low toxicity (Pant, B., et al., 2014; Pant B., et al., 2019). TiO_2 has three crystalline structures: rutile, anatase, and brookite (Allen, N.S., et al., 2018). The anatase and rutile phases are used in photocatalysis, while brookite is not very stable and its use is almost null (Zhang, J., et al., 2008; Di Paola, A., et al., 2013). On the other hand, silver has been used since ancient times as a bactericidal agent (Klasen H.J., 2000a; Klasen H.J., 2000b). Silver ions in silver nitrate and silver sulfadiazine are effective against gram-positive and gram-negative bacteria (Chen, R., et al., 2013; Mohiti-Asli, M., et al., 2014; Sun, Z., et al., 2016; Benli, B., and Yalin, C., 2017). The most important characteristic is its surface area, which enhances its antimicrobial action and the bioavailability of the materials used (Ying, J.Y., 2008). Heterogeneous materials are very important in recent years due to their photocatalytic activity (Fujishima, A.K., 1972; Hoffmann, M.S., et al., 1995; Somorjai, G.A., 1996; Mills, A., and Hunte, S.L., 1997; Burda, C., et al., 2005). When the anatase phase of TiO_2 is exposed to natural light, holes are generated and electrons are excited, the holes are trapped by water, and with this, hydroxyl radicals are generated that effectively degrade many of the organic pollutants (Carey, J., et al., 1976; Fujishima, A., et al., 2000; Nadtochenko, V., et al., 2005). However, because TiO_2 works under UV conditions (3.2 eV), doping with various metals has long been chosen to improve its sensitivity to visible light (Williamson, W.O., 1939; Anpo, M., et al., 2001; Asashi, R., et el., 2001; Khan, S.U.M., et al., 2002; Park, C.H., et al., 2002; Burda, C., et al., 2003; Yu, J.C., et al., 2005). Silver particles make it possible to activate the excitation in light of TiO_2 (Seery, M.K., et al., 2007). Silver nanoparticles increase the properties of TiO_2 and also this combination notably improves the antimicrobial properties of both materials, it is believed that silver improves the photoactivity of TiO_2 by reducing the recombination rate of its photo-excited charge carriers and/or by providing more surface area for adsorption (Sclafani, A., et al., 1997; Sung-Suh, H.M., et al., 2004). A large amount of silver released sometimes reduces antimicrobial activity (Wang, Y.L., 1998). So far there is not much information on the bacterial efficacy of cerium; however, very recently some syntheses were carried out including TiO_2 co-doped with silver and cerium, observing that under light or darkness this material eliminated more than 99.9% of E. Coli and S. Aureus and it was found that it could be used to eliminate bacteria (Moongraksathum, B., and Chen, Y., 2017).

In this work, the material will be synthesized using the sol-gel method, which consists of obtaining an oxide skeleton (metastable phase) by hydrolysis and polymerization at low temperatures, starting from a metallic alkoxide or inorganic salt.

EXPERIMENTAL METHODOLOGY

Synthesis of Ce/TiO_2

The synthesis was carried out by the sol-gel method from titanium butoxide, Ti $(OBu)_4$ (Sigma Aldrich> 97%); 12.8 mL of stereagent were mixed with 74.8 mL of ethanol and 76 mL of deionized water, and 2 and 4% (w / w) of $(NH_4)_2Ce(NO_3)_6$. The reagents were added in that order and they were homogenized with a magnetic stirrer for approximately 5 min, after this time they were emptied into 4 vials of the Anton Paar Synthos 3000 microwave reactor, in which they were synthesized under the following conditions: Maximum operating temperature 180 ° C, Reaction time 2 minutes, Ramp: 10 min. Subsequently, they were calcined for 24 h at 100 ° C.

Silver impregnation

Silver nitrate ($AgNO_3$) was mixed with water with constant stirring at 70 ° C. The $Ti_{1-x}Ce_xO_2$ powder was placed in a water bath at 70 ° C so that the impregnation with the $AgNO_3$ solution was carried out dropwise for 2 h; the $Ag/Ti_{1-x}Ce_xO_2$ powder was dried for 2 h at 200 °C, finally macerated and reduced for 3 hours at 400 °C.

Characterization of materials

The crystallinity of the solids was determined by X-ray diffraction using a SIEMENS D-500 diffractometer coupled to an X-ray tube, using a copper anode (CuKα radiation, λ = 1.54 nm). Scanning electron microscopy was performed on a JSM-6400 JEOL Noran Instruments SEM equipped for energy-dispersive X-ray spectroscopy (EDS). For the characterization of the textural properties, all the adsorption isotherms of N2 were determined at the boiling temperature of liquid nitrogen (-196.15 ºC; 77 K), using a fully automated volumetric adsorption system (ASAP 2000 from MICROMERITICS).

Antibacterial activity tests

To test the antimicrobial activity of the materials, strains of *Salmonella typhimurium* (ATCC 14028) were used, which were reseeded and stored at 4 °C (277.15 K) to maintain viability. The minimum inhibitory concentration (MIC) and minimum bactericidal concentration (MBC) of the materials were determined as bactericidal. To determine the inhibition kinetics of the bacteria, the average MBC of the materials will be exposed to bacteria contained in tubes with trypticasein soybean. Samples were taken at different times and were seeded in Petri dishes with McConkey agar by the plate striatum technique. The plates were incubated, inverted at 37 ° C for 24 hours in an aerobic atmosphere, and colony counting was carried out. As a control, a plate with a culture without bactericidal material was inoculated at the beginning and the end of each test.

RESULTS AND DISCUSSION

Figure 1 shows the diffractogram for the sample $Ag/Ti_{0.96}Ce_{0.04}O_2$, in this the crystalline phases of TiO_2-Ce and the deposits of Ag are identified. The diffraction pattern shows that the TiO_2 corresponds to the phase anatase with a minor fraction of the rutile phase.

Vol.7, No.2, pp.21-30, 2022
Print ISSN: 2397-7728(Print)
Online ISSN: 2397-7736(Online)

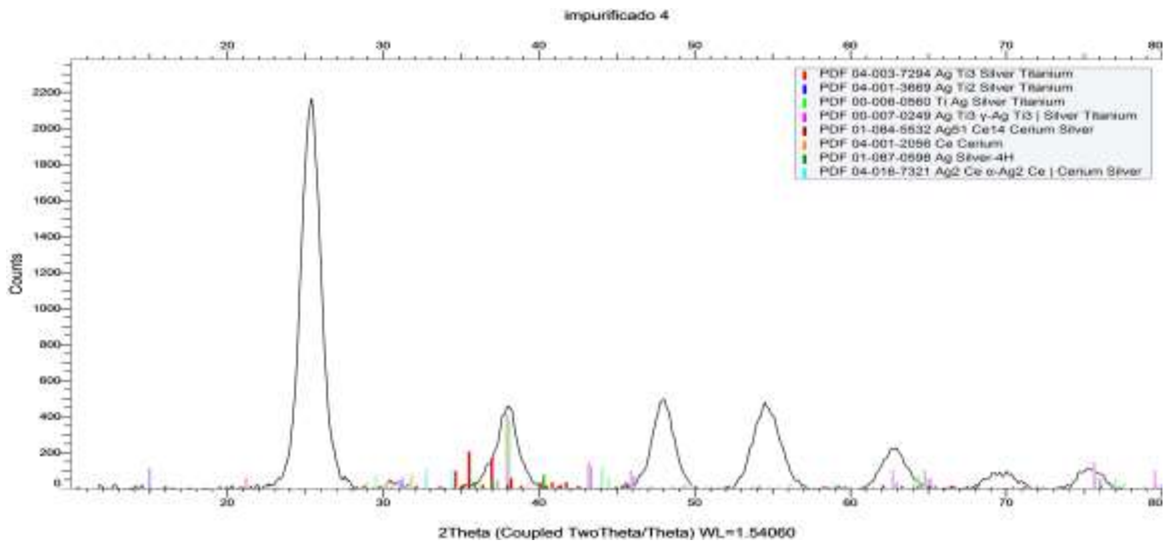

Figure 1. XR Diffraction result from the sample Ag/$Ti_{0.96}Ce_{0.04}O_2$

The morphology of the materials is presented in Figure 2. Figure 2a shows the micrographs of $Ti_{0.96}Ce_{0.04}O_2$ at 10000X; irregular particles with an average size of 0.5 nm and rough surface texture are observed, while the Ag/$Ti_{0.96}Ce_{0.04}O_2$, observed a smoother rough surface texture, which can be attributed to the heat treatment at 400 °C (673.15 K) to which the sample was subjected for 3 hours. Figure 3 shows the quantitative analysis of the field shown in figure 2, using the Energy Dispersive X-ray (EDS) technique; it is observed that the peak with the highest intensity corresponds to titanium, located at 4.5 keV.

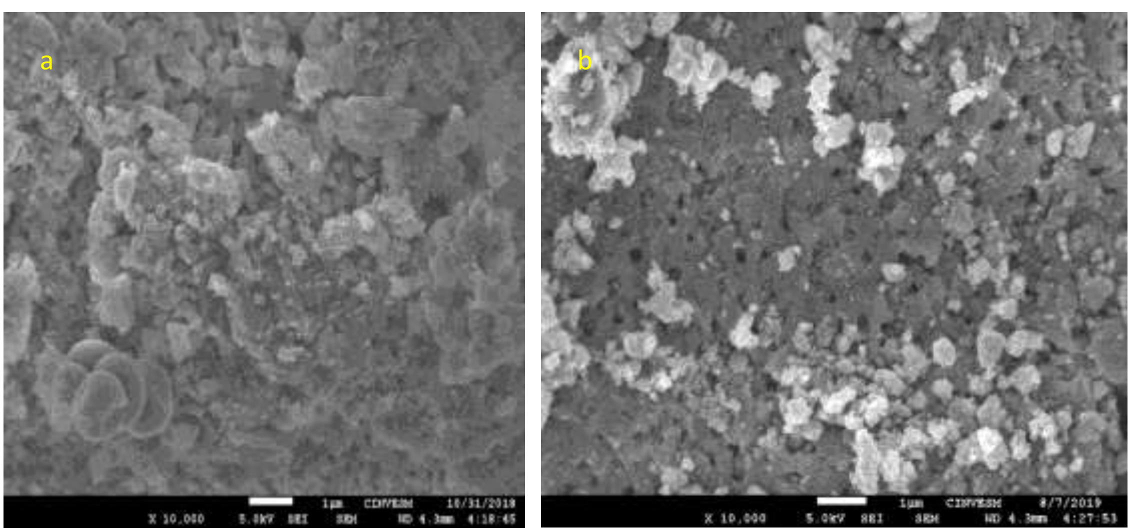

Figure 2. SEM Micrographs (10000X) of samples: a) $Ti_{0.96}Ce_{0.04}O_2$, and b) Ag/$Ti_{0.96}Ce_{0.04}O_2$

Print ISSN: 2397-7728(Print)
Online ISSN: 2397-7736(Online)

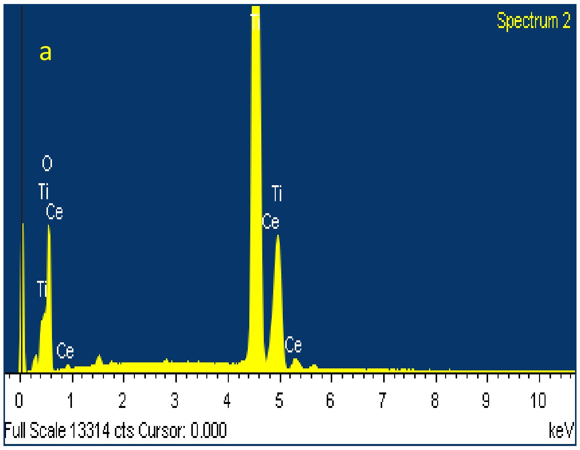

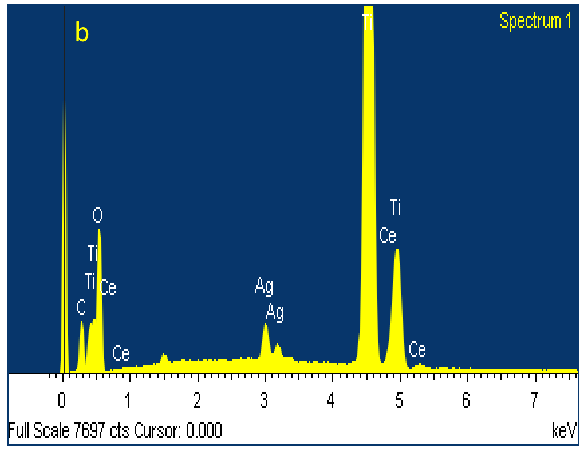

Figure 3. Energy Dispersive X-ray (EDS) images of samples: a) $Ti_{0.96}Ce_{0.04}O_2$, and b)Ag/$Ti_{0.96}Ce_{0.04}O_2$

The textural results (surface area and pore volume) obtained from the analysis of the N_2 isotherms at -196.15 ºC (77 K) have been evaluated using the BET equation, proposed by Brunauer, Emmett, and Teller (Brunauer, 1945). The results of these estimates are listed in Table 1. In turn, the mesopore size distribution has been evaluated by the Kelvin method (K), and the total pore volume is represented as the adsorbed volume close to saturation and it is calculated as the volume of liquid (Gurvitsch's Rule). According to the profile of the isotherms, they all correspond to a mesoporous solid; that is, the diameter of the pores is between 2 and 50 nm [17].

Table 1. Surface area, volume, and pore diameter values.

Sample	Surface area (m^2/g)	Pore diameter (nm)	Pore volume (cm^3/g)
TiO_2	130.99	5.68	0.236
$Ti_{0.96}Ce_{0.4}O_2$	183.76	10.152	0.466
Ag/$Ti_{0.96}Ce_{0.4}O_2$	182.76	8.72	0.398

Bacterial resistance tests

For bacterial resistance tests, MIC and MBC were determined according to NCCLS recommendations [18,19]. In the resistance tests, it is established that a MIC and MBC of $5.5x10^{-3}$ (g/mL) of Ag/$Ti_{0.96}Ce_{0.4}O_2$ is sufficient to inhibit the bacterial growth of *Salmonella typhimurium*, while for the determination of MBC it was considered a halo greater than 5 mm as negative.
Because the turbidimetric technique depends on the size of the bacterial cells as well as the presence of damaged cells [20], microbiological plating tests were performed to obtain

Vol.7, No.2, pp.21-30, 2022
Print ISSN: 2397-7728(Print)
Online ISSN: 2397-7736(Online)

bacterial growth or inhibition curves. Table 2 shows the results of the average of 3 bacterial growth or inhibition kinetics tests at 0, 20, 50, 90, and 120 minutes of exposure of the bacteria in the materials at 37 °C (310.15 K), 30 rpm, and varying the pH. The plates were incubated inverted at 37 ° C for 24 hours under an aerobic atmosphere and the colonies were counted. As a reference standard, a plate was inoculated with culture without bactericidal material.

Table 2. Colonies that survived exposure to the materials.

Material /time (min)		**pH=5±0.2**				**pH=6±0.2**				**pH=7±0.2**			
	0	**20**	**50**	**90**	**120**	**20**	**50**	**90**	**120**	**20**	**50**	**90**	**120**
Standard	152	155	176	189	218	158	176	194	229	160	179	201	235
TiO_2	152	153	165	171	182	155	163	168	179	155	168	172	192
$Ti_{0.96}Ce_{0.4}O_2$	152	145	161	162	158	153	159	160	162	145	155	151	148
$Ag/Ti_{0.96}Ce_{0.4}O_2$	152	84	35	21	1	98	42	15	0	84	35	18	0

Figure 4 shows the kinetic monitoring of the colonies that survived in the culture medium, in the presence of $Ag/Ti_{0.96}Ce_{0.4}O_2$, for the case of pH 5.0 to 7.0. The amount of $Ag/Ti_{0.96}Ce_{0.4}O_2$ sample was 0.05 g per 18 mL of culture media.

Vol.7, No.2, pp.21-30, 2022
Print ISSN: 2397-7728(Print)
Online ISSN: 2397-7736(Online)

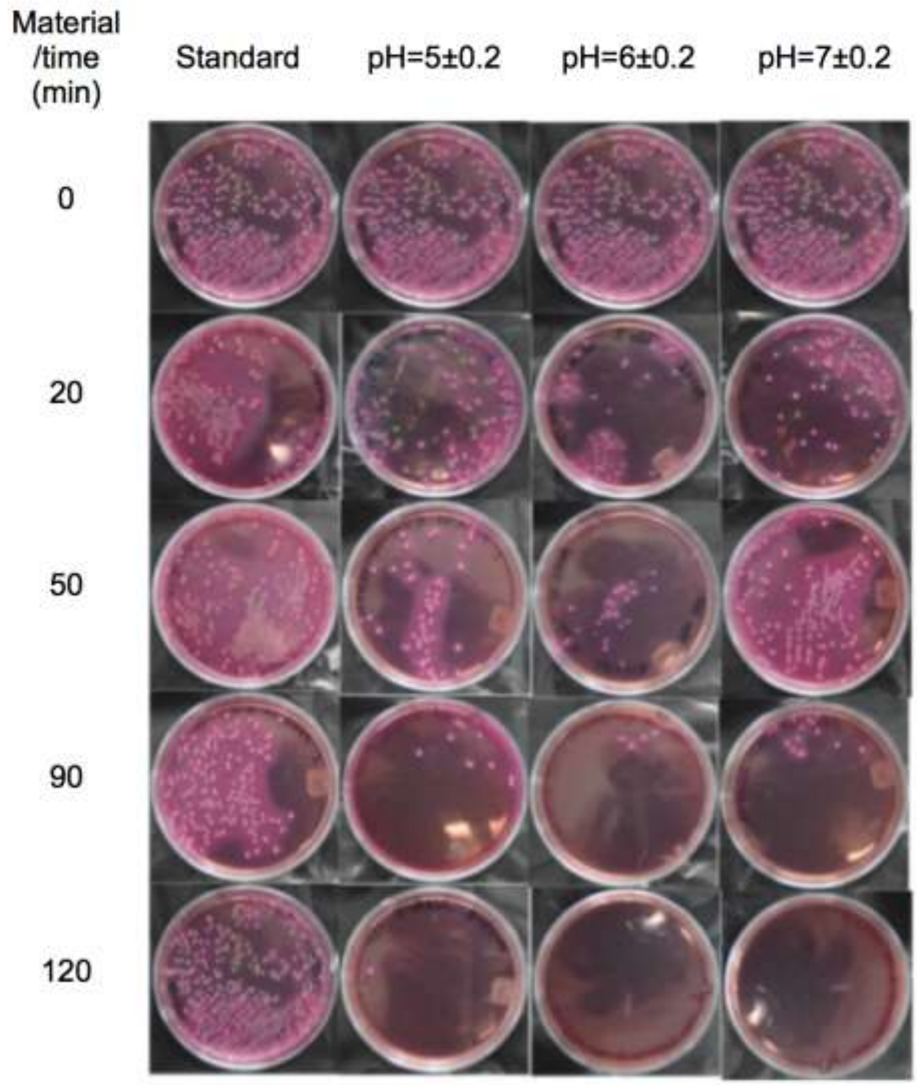

Figure 4. ***Salmonella Typhimurium*** **colonies that survived after the culture medium was in contact with Ag / $Ti_{0.96}Ce_{0.04}O_2$. The pH ranges from 5.0 to 7.0.**

The results of the bacteriological monitoring of the exposed materials show that the reference standard grows throughout the experiment, which indicates that the bacteria were not stressed by the change in pH in the nutrient medium. Bacteria in contact with the materials TiO_2 and $Ti_{0.96}Ce_{0.4}O_2$ showed a bacteriostatic behavior for up to 90 min, after which they observed an increase in this behavior. It is observed that the combination of Ti-Ce does not increase the bacterial population after 120 min, unlike the exposure with only Ti.

In solutions with slightly acidic pH, it is observed that the bacterial population has a slight tendency to decrease due to the effect of cerium, as reported by Soberk and Ta Iburt [15].

The $Ag/Ti_{0.96}Ce_{0.4}O_2$ material showed at all times the inhibition of the bacterium *Salmonella Typhimurium*, after 120 minutes this bacterium is eliminated.

CONCLUSIONS

From the experimental work of synthesis of a material based on TiO_2, doped with CeO_2, and covered with Ag, with the purpose to test its bactericidal effect against strains of *Salmonella Typhimurium*, the following conclusions are drawn:

The textural results of the silver nanoparticles supported on $Ti_{0.96}Ce_{0.4}O_2$, show the diameter of the pores in all samples ranges from 2 to 50 nm. The bacterial resistant tests show the combination of the elements Ti, Ce, and Ag in the $Ag/Ti_{0.96}Ce_{0.4}O_2$ worked as a bactericidal material for *Salmonella Typhimurium*, and the silver content of 4% (w/w) was sufficient to inhibit bacteria. This could be because cerium and titanium break down the cell membrane, which makes silver easily interact with the nucleus of bacteria.

Acknowledgment

The authors thank CONACyT for granting América Mondragón the scholarship No. 1007519 during her master's studies.

REFERENCES

Allen, N.S.; Mahdjoub, N.; Vishnyakov, V.; Kelly, P.J.; Kriek, R.J. The effect of crystalline phase (anatase, brookite, and rutile) and size on the photocatalytic activity of calcined polymorphic titanium dioxide (TiO2). Polym. Degrad. Stab. 2018, 150, 31–36.

Anpo, M., S. Kishiguchi, Y. Ichihashi, M. Takeuchi, H. Yamashita, K. Ikeue, B. Morin, A. Davidson, M. Che, Res. Chem. Intermediates 27 (2001) 459.

Asahi, R., T. Morikawa, T. Ohwaki, K. Aoki, Y. Taga, Science 293 (2001) 269.

Benli, B.; Yalın, C. The influence of silver and copper ions on the antibacterial activity and local electrical properties of single sepiolite fiber: A conductive atomic force microscopy (C-AFM) study. Appl. Clay Sci. 2017, 146, 449–456.

Burda, C., Y. Lou, X. Chen, A.C.S. Samia, J. Stout, J.L. Gole, Nano Lett. 3 (2003) 1049.

Burda, C., X. Chen, R. Narayanan, M.A. El-Sayed, Chem. Rev. 105 (2005) 1025.

Carey, J., J. Lawrence, H. Tosine, Bull. Environ. Contam. Toxicol. 16 (1976) 697.

Chen, R.; Ni, H.; Zhang, H.; Yue, G.; Zhan, W.; Xiong, P. A preliminary study on antibacterial mechanisms of silver ions implanted stainless steel. Vacuum 2013, 89, 249–253.

Di Paola, A.; Bellardita, M.; Palmisano, L. Brookite, the Least Known TiO2 Photocatalyst. Catalysts 2013, 3, 36–73.

Fenwick, A. Waterborne Diseases—Could they be Consigned to History? Science 2006, 313, 1077–1081.

Fujishima, A., K. Honda, Nature 238 (1972) 37.

Fujishima, A., N.R. Tata, A. Tryk, J. Photochem. Photobiol. C 1 (2000) 1.

George, I.; Crop, P.; Servais, P. Use of β-D-Galactosidase and β-D-Glucuronidase Activities for Quantitative Detection of Total and Faecal Coliforms in Wastewater. Can. J. Microbiol. 2001, 47, 670–675.

Grabow, W.O.K. Waterborne Diseases: Update on Water Quality Assessment and Control. Water SA 1996, 22, 193–202.

Hoffmann, M.S., T. Martin, W. Choi, D.W. Bahnemann, Chem. Rev. 95 (1995) 69.

Khan, S.U.M., M. Al-Shahry, W.B. Ingler Jr., Science 297 (2002) 2243.

Klasen, H.J. Historical review of the use of silver in the treatment of burns. I. Early uses. Burn. J. Int. Soc.Burn Inj. 2000a, 26, 117–130.

Klasen, H.J. A historical review of the use of silver in the treatment of burns. II. Renewed interest for silver. Burns 2000b, 26, 131–138.

Liou, J. W. & Chang, H. H. Bactericidal effects and mechanisms of visible light-responsive titanium dioxide photocatalysts on pathogenic bacteria. Archivum immunologiae et therapiae experimentalis 60, 267–275 (2012).

McDonnell, G. & Russell, A. D. Antiseptics and disinfectants: activity, action, and resistance. Clinical microbiology reviews 12,147–179 (1999).

Mills, A., S.L. Hunte, J. Photochem. Photobiol. A 108 (1997) 1.

Mohiti-Asli, M.; Pourdeyhimi, B.; Loboa, E.G. Novel, silver-ion-releasing nanofibrous scaffolds exhibit excellent antibacterial efficacy without the use of silver nanoparticles. Acta Biomater. 2014, 10, 2096–2104.

Moongraksathum B. & Chen Y., Anatase TiO2 co-doped with silver and ceria for antibacterial application. Catalysis Today. 2017, 6.

Nadtochenko, V., A. Rincon, S. Stanca, J. Kiwi, J. Photochem. Photobiol. A 169 (2005) 131.

Opoku, F.; Govender, K.K.; van Sittert, C.G.C.E.; Govender, P.P. Recent Progress in the Development of Semiconductor-Based Photocatalyst Materials for Applications in Photocatalytic Water Splitting and Degradation of Pollutants. Adv. Sustain. Syst. 2017, 1, 1700006.

Pant, B.; Barakat, N.A.M.; Pant, H.R.; Park, M.; Saud, P.S.; Kim, J.-W.; Kim, H.-Y. Synthesis and photocatalytic activities of CdS/TiO2 nanoparticles supported on carbon nanofibers for high efficient adsorption and simultaneous decomposition of organic dyes. J. Colloid Interface Sci. 2014, 434, 159–166.

Pant, B.; Park, M.; Kim, H.-Y.; Park, S.-J. Ag-ZnO photocatalyst anchored on carbon nanofibers: Synthesis, characterization, and photocatalytic activities. Synth. Met. 2016, 220, 533–537.

Pant, B.; Park, M.; Park, S.-J. Hydrothermal synthesis of Ag2CO3-TiO2 loaded reduced graphene oxide nanocomposites with highly efficient photocatalytic activity. Chem. Eng. Commun. 2019, 1–8.

Park, C.H., S.B. Zhang, S.H. Wei, Phys. Rev. B 66 (2002) 073202.

Sclafani, A., M.N. Mozzanega, J.M. Herrmann, J. Catal. 168 (1997) 117.

Seery, M.K., R. George, P. Floris, S.C. Pillai, J. Photochem. Photobiol. A 189 (2007) 258.

Sung-Suh, H.M., J.R. Choi, H.J. Hah, S.M. Koo, Y.C. Bae, J. Photochem. Photobiol. A 163 (2004) 37.

Somorjai, G.A., Chem. Rev. 96 (1996) 1223.Sun, Z.; Fan, C.; Tang, X.; Zhao, J.; Song, Y.; Shao, Z.; Xu, L. Characterization and antibacterial properties of porous fibers containing silver ions. Appl. Surf. Sci. 2016, 387, 828–838.

Wang, Y.L., Y.Z. Wan, X.H. Dong, G.X. Cheng, H.M. Tao, T.Y. Wen, Carbon 36 (1998) 1567.

WHO (World Health Organization). Guidelines for Drinking-water Quality, Incorporating 1st and 2nd Addenda, Volume 1, Recommendations, 3rd ed.; WHO: Geneva, Switzerland, 2008.

Williamson, W.O., Nature 143 (1939) 279.

Ying, J.Y. The era of nanotechnology. Nano Today 2008, 3, 1.

Yu, J.C., W. Ho, J. Yu, H. Yip, P.K. Wong, J. Zhao, Environ. Sci. Technol. 39 (2005) 1175.

Zhang, J.; Xu, Q.; Feng, Z.; Li, M.; Li, C. Importance of the Relationship between Surface Phases and Photocatalytic Activity of TiO2. Angew. Chem. 2008, 120, 1790–1793.